Wind extremes in the North Sea Basin under climate change: An ensemble study of 12 CMIP5 GCMs

R. C. de Winter,[1,2] A. Sterl,[2] and B. G. Ruessink[1]

[1] Coastal safety may be influenced by climate change, as changes in extreme surge levels and wave extremes may increase the vulnerability of dunes and other coastal defenses. In the North Sea, an area already prone to severe flooding, these high surge levels and waves are generated by low atmospheric pressure and severe wind speeds during storm events. As a result of the geometry of the North Sea, not only the maximum wind speed is relevant, but also wind direction. Climate change could change maximum wind conditions, with potentially negative effects for coastal safety. Here, we use an ensemble of 12 Coupled Model Intercomparison Project Phase 5 (CMIP5) General Circulation Models (GCMs) and diagnose the effect of two climate scenarios (rcp4.5 and rcp8.5) on annual maximum wind speed, wind speeds with lower return frequencies, and the direction of these annual maximum wind speeds. The 12 selected CMIP5 models do not project changes in annual maximum wind speed and in wind speeds with lower return frequencies; however, we do find an indication that the annual extreme wind events are coming more often from western directions. Our results are in line with the studies based on CMIP3 models and do not confirm the statement based on some reanalysis studies that there is a climate-change-related upward trend in storminess in the North Sea area.

1. Introduction

[2] Low-lying coastal areas around the North Sea have encountered severe flooding throughout history, with the most recent events in 1953 in the south-west of the Netherlands, Belgium, and England, and in 1962 in the German Bight. These floodings were caused by extreme high storm surge levels in combination with extreme waves, the 1953 event, for example, had a return period of approximately 1:1000 year [*Sterl et al.*, 2009]. In the North Sea, these high surge levels and waves are generated by low atmospheric pressure and severe wind speeds during storm events. As a result of the geometry of the North Sea basin, not only the maximum wind speed is relevant, but also the associated direction. For the Dutch coast, winds coming from north-north-west have the largest

fetch and can therefore generate large waves and storm surges, while for the German Bight, winds from west-north-west have the largest fetch. A change in wind direction of the extreme wind will thus affect coastal areas in the North Sea in a different manner.

[3] The extreme wind speed in the current wind climate in the north-east Atlantic Ocean has a considerable interdecadal and interannual variability [*WASA-Group*, 1998]. Studies based on sea level pressure observations show a peak in intensity in geostrophic wind at the beginning and at the end of the 20th century, a dip in intensity in the 1960s, without an upward or downward trend [*Alexandersson et al.*, 1998, 2000; *Wang et al.*, 2011]. Both studies used 95th and 99th percentiles per year to derive measures of storminess and the corresponding occurrence frequencies. *Alexandersson et al.* [1998, 2000] used observations covering 1881 to 1995 and 1998, respectively, *Wang et al.* [2011] used observational data covering 1878–2007 from the International Surface Pressure Bank. *Donat et al.* [2011] based their findings on pressure fields from the 20th Century Reanalysis (20CR) [*Compo et al.*, 2011] running from 1871 to 2008 and suggest an upward trend in storminess, with an increase in occurrence frequency of strong geostrophic wind. They suggest a climate-change-related upward trend in storminess in the North Sea area. (O. Krueger, F. Schenk, F. Feser, and R. Weisse, Inconsistencies between long-term trends in storminess derived from the 20CR reanalysis and observations, J. Climate, in press, doi:10.1175/JCLI-D-12-00309.1) recently debated whether this upward trend in storminess

[1]Department of Physical Geography, Faculty of Geosciences, Institute for Marine and Atmospheric Research, Utrecht University, P.O. Box 80.115, 3508 TC Utrecht, Netherlands.
[2]Royal Netherlands Meteorological Institute (KNMI), P.O. Box 201, 3730 AE De Bilt, Netherlands.

Corresponding author: R. C. de Winter, Department of Physical Geography, Faculty of Geosciences, Institute for Marine and Atmospheric Research, Utrecht University, P.O. Box 80.115, 3508 TC Utrecht, Netherlands. (r.c.dewinter@uu.nl)

is actually present for the last decade, as they noted winds based on 20CR to be inconsistent with observations at the beginning of the 20th century. Moreover, the interdecadal variability is large which hampers statements that an upward trend, if present, is the result of anthropogenic climate change or of the interdecadal variability.

[4] Studies that analyzed extreme wind speed in a future climate do not show significant changes [*Van den Hurk et al.*, 2007; *Nikulin et al.*, 2011; *Pryor et al.*, 2012]. These three studies analyzed annual maximum events and corresponding return values, based on two to six Coupled Model Intercomparison Project Phase 3 (CMIP3) General Circulation Models (GCMs) They all compare their results with the 1961–1990 historical period. *Van den Hurk et al.* [2007] analyzed three SRES scenario, for the period 2081–2100 and the periods 2181–2200, 2281–2300 if data was available. *Nikulin et al.* [2011] and *Pryor et al.* [2012] used SRES A1b for the period 2071–2100, and 2036–2065 and 2070–2099, respectively. The analysis of wind extremes in the 17-member ESSENCE ensemble [*Sterl et al.*, 2009], based on SRES A1b, comparing period 1950–2000 with 2050–2100, confirmed that the magnitude of the extreme wind speed, with return periods up to 1 in 10,000 year, was not projected to change. However, they did project a shift in wind directions, with more extreme winds from western directions.

[5] Analyzing changes in a changing climate implies that several uncertainties need to be taken into account [*Hawkins and Sutton*, 2009]. First, there is the uncertainty in emission scenarios, which represent the possible development of greenhouse gas emission. Second, there is uncertainty between the climate models that are used to analyze the effect of different climate scenarios. The third uncertainty is the natural variability of the climate. When this system variability is large, small trends will be difficult to detect, especially for events with high return values. The effect of this natural variability on uncertainty when projecting high return values can be reduced by using an ensemble of one model with different initial conditions, as, in a coastal context, performed with the ESSENCE-ensemble by *Sterl et al.* [2009] for storm surge levels and *De Winter et al.* [2012] for extreme waves in the North Sea.

[6] In this paper, we examine possible changes in the magnitude of annual maximum wind extremes and the corresponding wind directions as a result of climate change. We analyze the effect of two emission scenarios (rcp4.5 and rcp8.5) to address the effect of different developments of greenhouse gases. Rcp4.5 is considered to be a middle emission scenario, while rcp8.5 represents high-end climate scenarios [*Meinshausen et al.*, 2011]. We use 12 CMIP5 GCMs to determine if there is consensus, in projecting future wind characteristics. We focus on the North Sea basin, because changes in wind conditions could have a large impact on safety of the generally densely populated North Sea coast, an area that has already a high exposure to flooding [*Parry et al.*, 2007]. The difference between the historical run and the scenarios rcp4.5 and rcp8.5 highlights climate-change-induced changes in annual extreme wind conditions in the North Sea. In particular, we clarify if the projections in CMIP5 of annual maximum wind speed and wind direction, and the wind speed with return values up to 500 years, for the North Sea basin have changed with respect to those in the CMIP3 models.

Table 1. CMIP5 Models Used in Present Study and Their Resolution[a]

Model	No. of Ensembles Members			Longitude	Latitude
	Historical	rcp4.5	rcp8.5	$\Delta\lambda$	$\Delta\varphi$
CanESM2	5	5	5	2.8125	2.8125
CSIRO-Mk3-6-0	5	1	1	1.875	1.875
EC-Earth	1	1	1	1.125	1.125
GFDL-ESM2G	1	1	1	2.5	2.0
GFDL-ESM2M	1	1	1	2.5	2.0
HadGEM2-CC	3	1	3	1.875	1.25
HadGEM2-ES	1	1	1[b]	1.875	1.25
IPSL-CM5A-MR	1	1	1	2.5	1.25
MIROC-ESM-CHEM	1	1	1	2.8125	2.8125
MIROC5	4	3	3	1.40625	1.41
MPI-ESM-LR	3	3	3	1.875	1.875
MRI-CGCM3	1	1	1	1.125	1.125

[a]More information is available on-line (http://cmip-pcmdi.llnl.gov/cmip5). $\Delta\lambda$ and $\Delta\varphi$ are the increments in longitudinal and meridional direction, respectively, in degrees. The increments in latitudinal direction are averages as some models use nonconstant (e.g., Gaussian) latitudes.
[b]Data available from 2076 to 2100.

2. Methods

2.1. Data

[7] Our work is based on daily northward and eastward surface wind (u_{as} and v_{as}) from 12 CMIP5 GCMs (Table 1). Daily mean u_{as} and v_{as} were considered to be adequate for our work. Since, severe storm surge levels and extreme waves only develop for severe winds blowing substantially longer than 3 h. For each of these models, we used a historical run
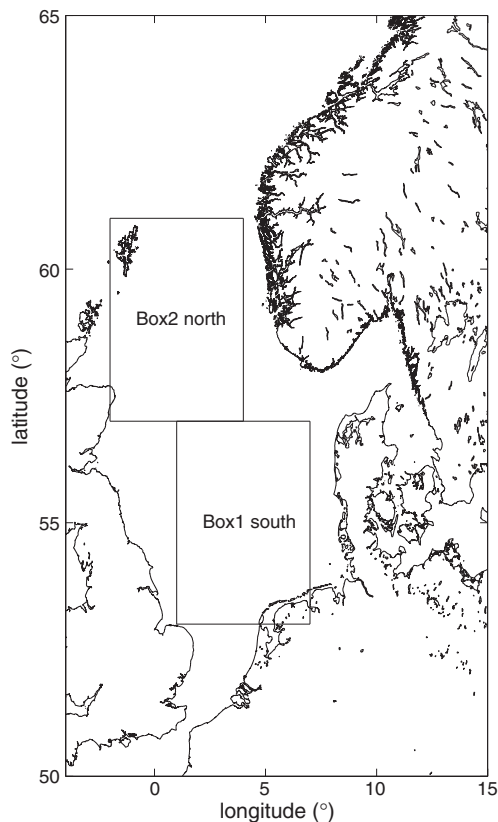

Figure 1. North Sea boxes.

(1950–2000) and two future scenarios (2050–2100): rcp4.5 and rcp8.5, where rcp stands for Representative Concentration Pathway (rcp). Rcp4.5 has a moderate increase in greenhouse gases, while rcp8.5 represents high-end climate scenarios [*Meinshausen et al.*, 2011]. The resolution of the GCMs was roughly between 1° and 3°, see Table 1 for details.

[8] Per model and scenario the annual maximum (anmx) wind speed $\left(U_{as}^{anmx}\right)$ was selected according to: $U_{as}^{anmx} = \max\left(\sqrt{u_{as}^2 + v_{as}^2}\right)$. For each U_{as}^{anmx}, the corresponding u$_{as}$ and v$_{as}$ were used to calculate the wind direction.

[9] We chose to use 50 year time slices to be able to deal with the large interannual variability in wind characteristics. For some models, an ensemble based on different initial conditions was available; an overview of the number of ensemble members per model and per scenario is given in Table 1. For model–scenario combinations with more than one member, all members together were analyzed as a single data set, extending the number of years in those model–scenario combinations (e.g., for a run with one member, this is 50 years, for a run with five members, this is $5 \times 50 = 250$ years). Small perturbations in the initial conditions ensure that every ensemble member evolves differently; however, the rcp is the same for the different members. One could argue that the use of 50 year time slices masks nonstationarity in annual extreme wind characteristics. As a check, we analyzed the differences for 2050–2070 relative to 2080–2100 for both scenarios, using the GCMs where multiple ensembles were available

(otherwise, the amount of years is too low to deal with interannual variability). For both scenarios, U_{as}^{anmx} for the period 2050–2070 did not differ from those in the period 2080–2100. This implies that there is no indication for nonstationarity and that the use of 50 year time period is justified.

2.2. Annual Maxima and Return Values

[10] The annual maximum conditions were analyzed per model and scenario. For the North Sea, changes in the mean U_{as}^{anmx} were studied for each GCM by calculating the difference in mean U_{as}^{anmx} between the future and the historical period. This allowed us to diagnose consistency of spatial patterns in U_{as}^{anmx} changes between the different models.

[11] Subsequently, we performed an Extreme Value (EV) analysis, based on annual maximum values within two predefined areas. As the selected GCMs have different grid resolutions, we decided to aggregate the North Sea into two boxes: Box 1 (North) 57°N–61°N,2°W–4°E and Box 2 (South) 53°N–57°N,1°E–7°E, see Figure 1. Each box covered several grid cells, with the precise number of cells varying per GCM. Accordingly, the boxes served as search windows: for each year, the maximum U_{as}^{anmx} was selected, resulting in a representative maximum value for each box per year. As wind speed over sea is usually larger than wind speed over land, searching for the maximum out a box automatically excluded grid cells that were partly within a box, but also partly above land. This is desirable as our primary motivation for this work relates to waves and surges.
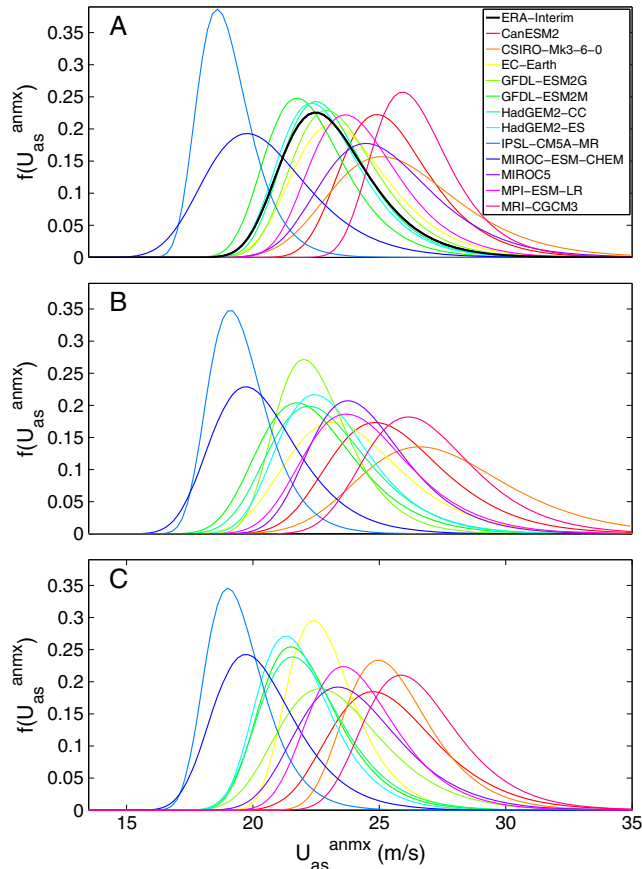

Figure 2. The Gumbel PDFs of U_{as}^{anmx} for the northern box. (a) Historical period and ERA-Interim, (b) rcp4.5, and (c) rcp8.5. Legend in Figure 1a applies to all panels.
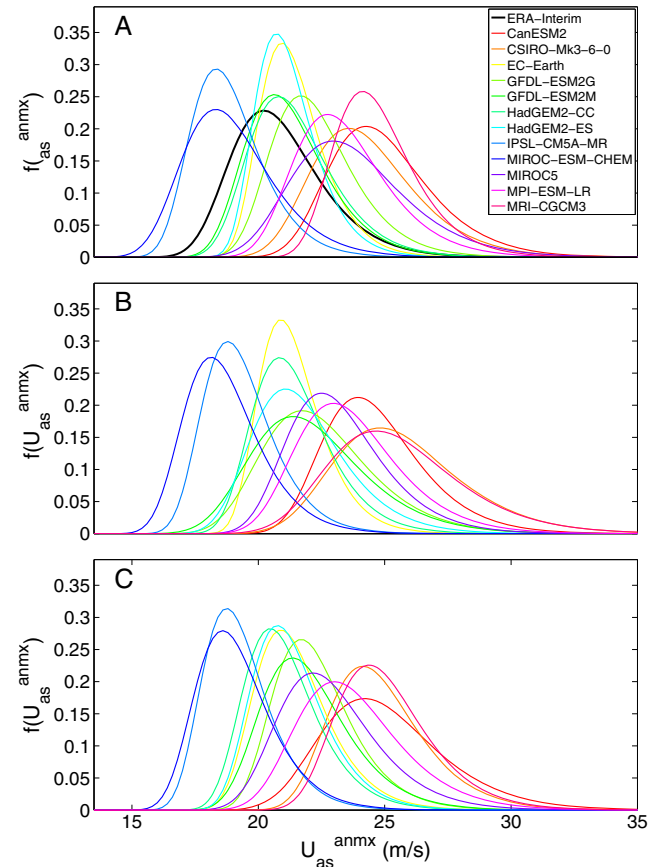

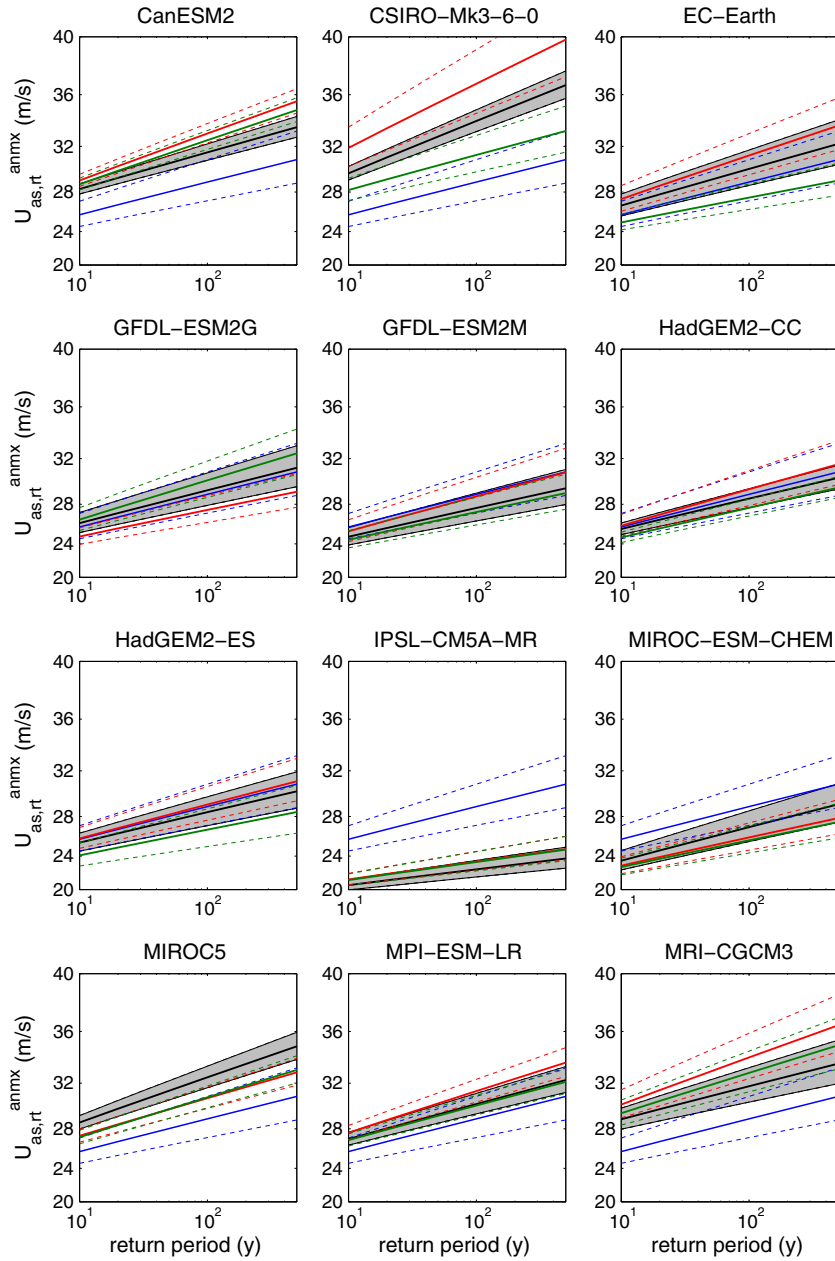**Figure 3.** As Figure 2, now for southern box.

Figure 4. The return values per model for ERA-Interim, blue; the historical period, black; and the two scenarios, rcp4.5, red; and rcp8.5, green in the northern box. The 95% confidence levels are depicted in dotted lines of the same color and for the historical run in gray shading.

[12] *Van den Brink and Können* [2008] showed that for relatively short record lengths of parameter *y*, EV statistics can be determined more accurately by fitting a Gumbel distribution, rather than a Generalized EV (GEV) distribution, to the annual maxima of *y* to avoid the large sensitivity of the GEV to the largest value of *y*. They further showed that even better results were obtained by fitting the Gumbel distribution to y^k, where *k* is based on the Rayleigh distribution of the whole wind data. With this method, the total wind speed record is thus assumed to have a particular shape, which is particularly relevant for the shape of the tail of the distribution and avoids the sensitivity to a single large value.

[13] For the North Sea, a value of *k* = 2 is appropriate for analyzing wind conditions. Following *Van den Brink and*

Können [2008], we fitted a Gumbel distribution to $\left(U_{as}^{anmx}\right)^2$, obtaining the location (μ) and scale parameter (σ), and the 95% confidence intervals of this distribution. The fit was performed using the "evfit" function from the Statistical Toolbox in Matlab R2010b. The Probability Density Function (PDF) of the EV was determined with "gevpdf" of the Statistical Toolbox, following [*Coles*, 2001]:

$$f\left(\left(U_{as}^{anmx}\right)^2 : \mu, \sigma\right) = \frac{1}{\sigma} exp\left[-exp\left(-\frac{\left(U_{as}^{anmx}\right)^2 - \mu}{\sigma}\right) \\ -\frac{\left(U_{as}^{anmx}\right)^2 - \mu}{\sigma}\right] \quad (1)$$
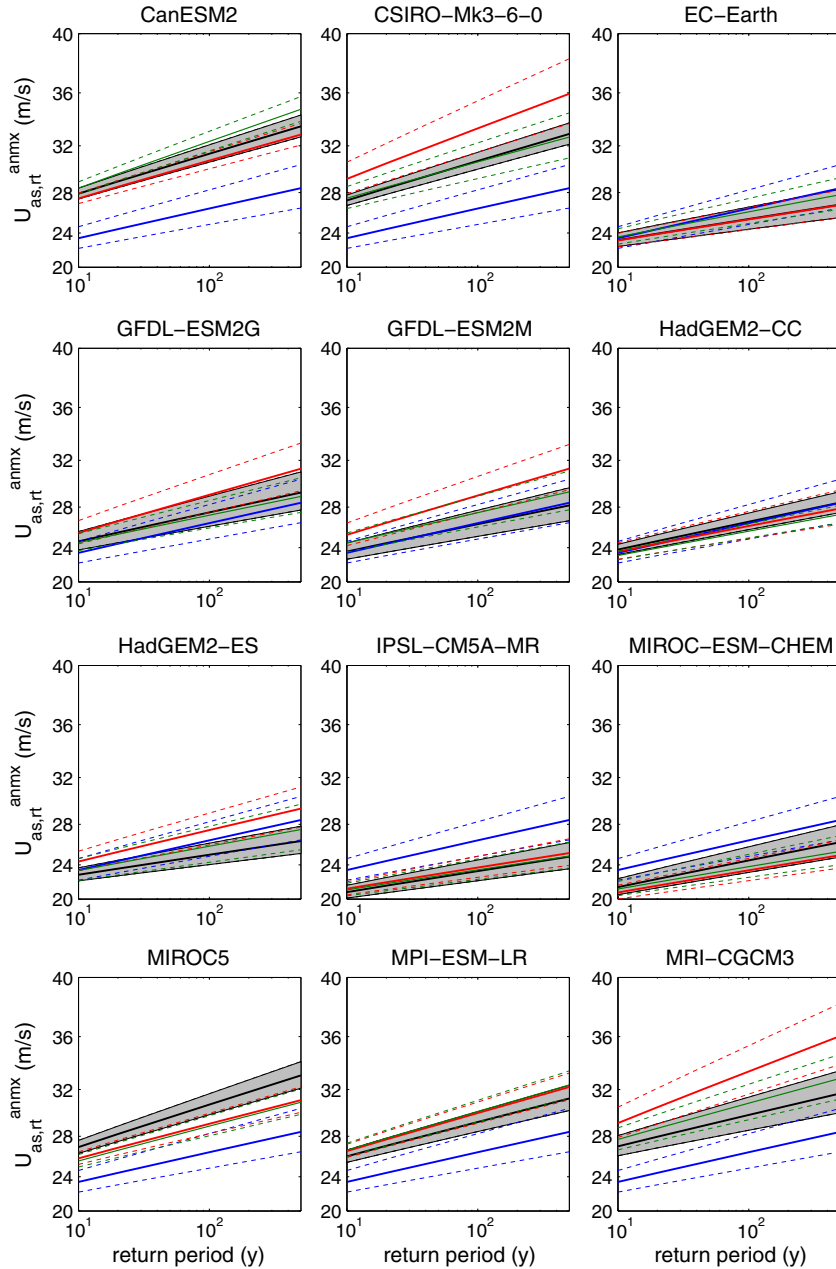
Figure 5. As Figure 4, now for southern box.

[14] The location of the peak of the PDF is determined by μ, while σ influences the width of the PDF. The same parameters were also used to calculate the t-year return values for U_{as}^{anmx}:

$$U_{10,rt}^{anmx}(t) = \sqrt{\mu - \sigma \log\left[-\log\left(1 - \frac{1}{t}\right)\right]}. \qquad (2)$$

[15] The bandwidth of the return values was calculated using the parameters for the 95% confidence interval, and equation (2).

2.3. Wind Direction

[16] The changes in the wind direction of U_{as}^{anmx} were examined for the center of each box, being 59°N, 1°E, and 55°N, 4°E. Per model and scenario, the wind directions were analyzed in bins of 22.5°, resulting in 16 wind directions. Per wind direction, we determined how often, as percentage of time, the annual maximum wind was coming from that direction (%$_{wind}$). This %$_{wind}$ per direction were based on a limited amount of data (50 to 250 years depending on the model). To determine the statistical robustness of these %$_{wind}$ per wind direction, the wind directions per model and scenario were bootstrapped [*Von Storch and Zwiers*, 2001] with a sample size of 1000. For these 1000 solutions, the %$_{wind}$ per direction was again calculated. This resulted in a series of %$_{wind}$ per direction, from which we determined the standard deviation (*sd*) per model, scenario, and directional bin.

[17] For each model, changes in the wind directions were determined by subtracting %$_{wind}$ of the historical run from the two future runs. The *sd* of the historical run

was used to provide information about the size of the statistical uncertainty.

3. Results

3.1. GCMs and ERA-Interim Wind Extremes

[18] We are primarily interested in relative differences between the historical and future period. Before we examine the climate-change-induced change in wind characteristics in the GCMs, we first focus on the performance of the historical period relative to the current wind climate. To this end, we compare the results of the historical runs with ERA-Interim, a climate reanalysis with assimilated observed wind data [*Dee et al.*, 2011] covering the period 1979–2011. This period is shorter than the 50 years of our historical run (1950–2000) and also does not fully overlap. Therefore, the comparison of the historical runs with ERA-Interim should be seen as an indication of the performance of the CMIP5 models. For the comparison with ERA-Interim, we use the same search windows defined in section 2.2 to select U_{as}^{anmx}. For both boxes, we compare the magnitude of U_{as}^{anmx} by comparing the fitted Gumbel PDF for the historical run of the 12 models with that of ERA-Interim, see top panels of Figures 2 and 3. Furthermore, we compare the return values of ERA-Interim with the return values we obtain for the historical runs, see Figures 4 and 5. The confidence intervals of the historical run in these figures are potentially influenced by the number of ensemble members of the models, as more members increase the amount of years and reduce the statistical uncertainty. Therefore, more members could result in narrower uncertainty bands.

[19] The PDF of ERA-Interim confirms the well-known fact of large interannual variability of U_{as}^{anmx} [*WASA-Group*, 1998; *Alexandersson et al.*, 2000; *Donat et al.*, 2011; *Wang et al.*, 2011]. The PDFs of the historical run also demonstrate this large interannual variability. Although all model PDFs are around the PDF of ERA-Interim, some model PDFs do show a large discrepancy relative to ERA-Interim. For six of the 12 GCMs, the return values of the historical run overlap with the 95% confidence interval of ERA-Interim, while the return values of the historical run of four (one) models are higher (lower) than the return values of ERA-Interim, see Figures 4 and 5. For one GCM, the return values of the northern area overlaps with ERA-Interim, whereas the return values of the southern area are higher than those of ERA-Interim. The grid resolution of the GCMs (Table 1) appears to be unrelated to the performance of the GCMs relative to ERA-Interim.

[20] We also compare the wind direction in the historical run with the wind directions in ERA-Interim by calculating how often, as percentage of time, U_{as}^{anmx} is coming from each direction in 22.5° wide bins. Subsequently, we analyze these percentages for all individual models relative to the percentages in ERA-Interim. Figure 6 shows for the northern location that U_{as}^{anmx} is coming from all directions with a peak in annual extreme winds from south-east. The southern location has most U_{as}^{anmx} from south-south-west to north-north-west. In general, the historical runs of the GCMs project the same dominant directions as ERA-Interim; in more detail, winds from north-west and north-north-west are less present in the historical runs of the GCMs than in ERA-Interim.
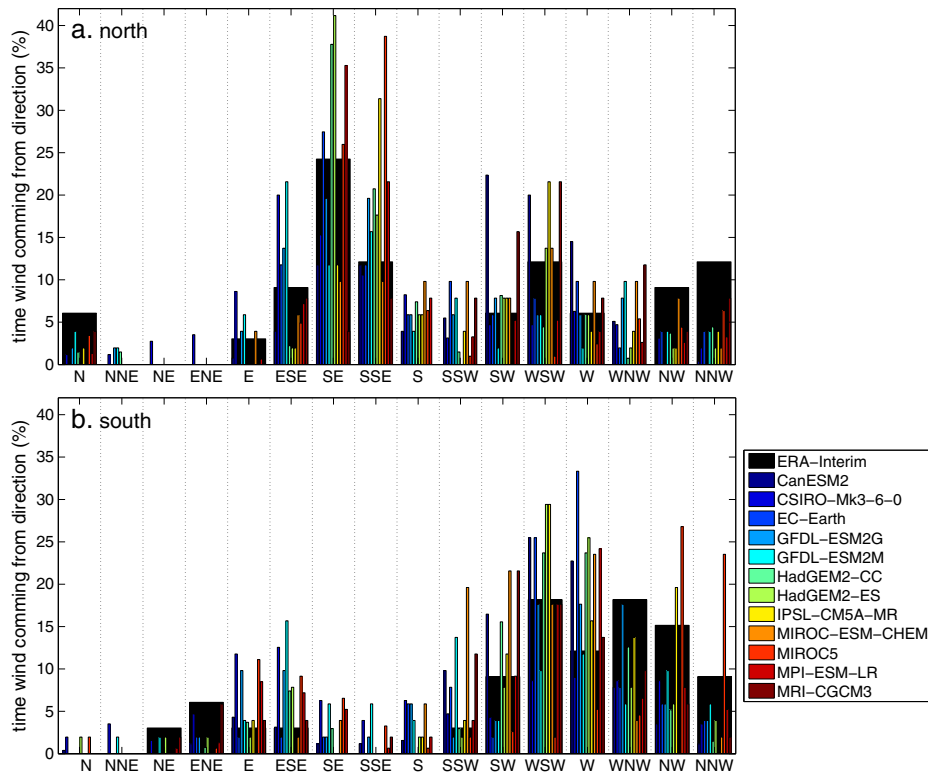

Figure 6. The percentage of U_{as}^{anmx} per direction for ERA-Interim and the historical runs. (a) Northern location, (b) southern location.

3.2. Changes in Maximum Wind Speed

[21] We diagnose changes in mean U_{as}^{anmx} by comparing the historical runs with the two future scenarios. First, we discuss changes in the total North Sea basin. Second, we study the PDF and return values of the EV analysis for the two boxes in Figure 1.

[22] Figure 7 demonstrates that the mean U_{as}^{anmx} of rcp8.5 and the historical run are not projected to differ much for the North Sea basin. For all models, the maximum difference is around 1 m/s. Furthermore, no consistent spatial pattern can be detected in Figure 7. Results based on rcp4.5 are similar (not shown), with again the largest difference around 1 m/s and the absence of a spatial pattern between models.

[23] Figures 2 and 3 depict the PDFs of the (a) historical run and the two future runs, (b) rcp4.5 and(c) rcp8.5. The models differ hugely in PDFs. The differences between the models are larger than the differences between scenarios for a given model, compare top and bottom panels in Figures 2 and 3. To see whether the models project a systematic change in U_{as}^{anmx} depending on climate scenario, we analyze the PDFs for each model. There is, however, no consisted shift in PDFs between the GCMs (Figures 8 and 9). This is also evident from Figures 4 and 5 where the confidence intervals of most of the annual maximum events (return period 10^1 years) of the future projections lie within the confidence interval of the historical run. An exception is the southern location of CSIRO-Mk3-6-0,
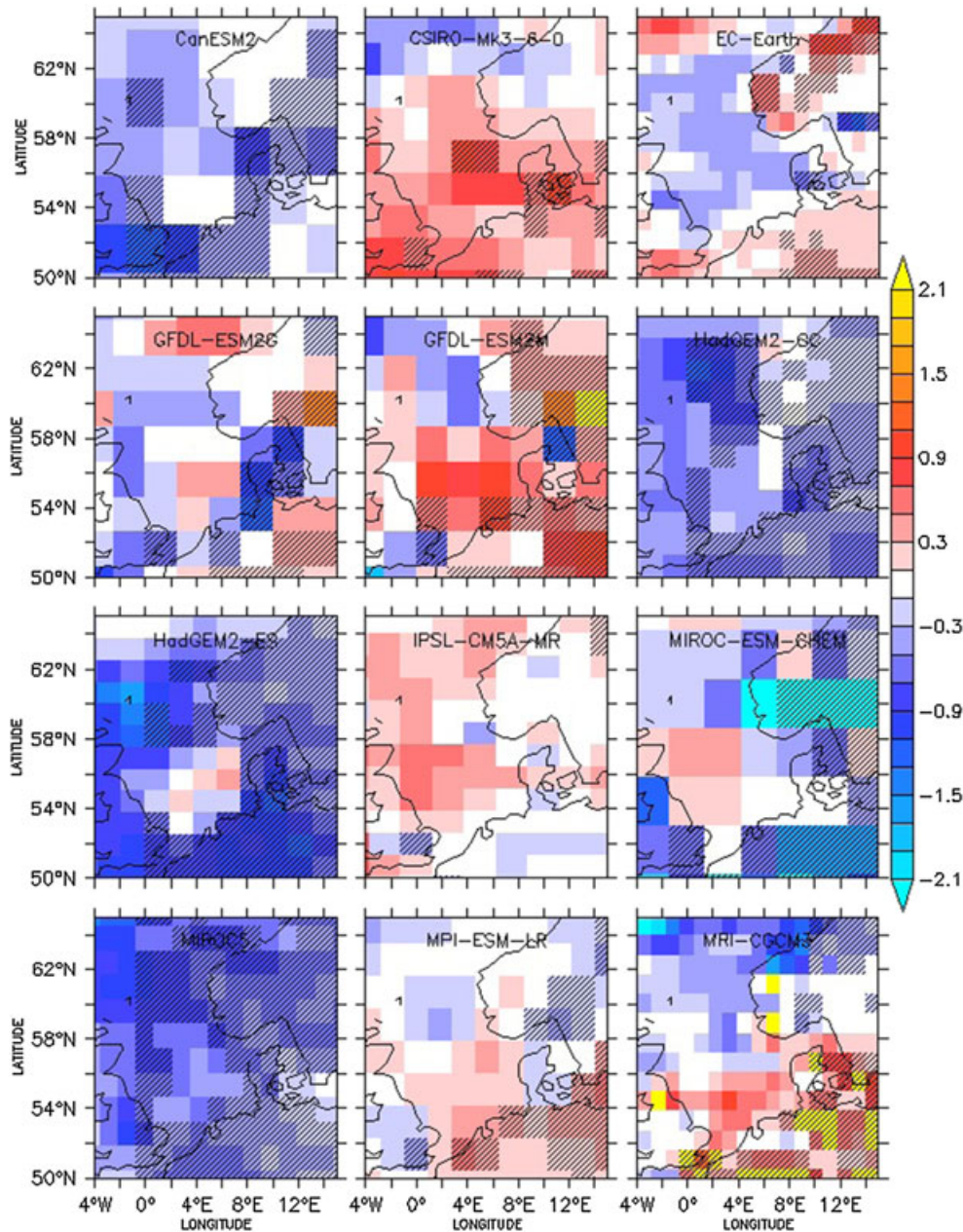

Figure 7. The difference in U_{as}^{anmx} (m/s) between rcp8.5 and the historical run for each model. The difference is significant according the 95% confidence interval for the shaded areas. The land contour in this figure are an indication of the actual land contour and are not related to the land–sea mask of the model.
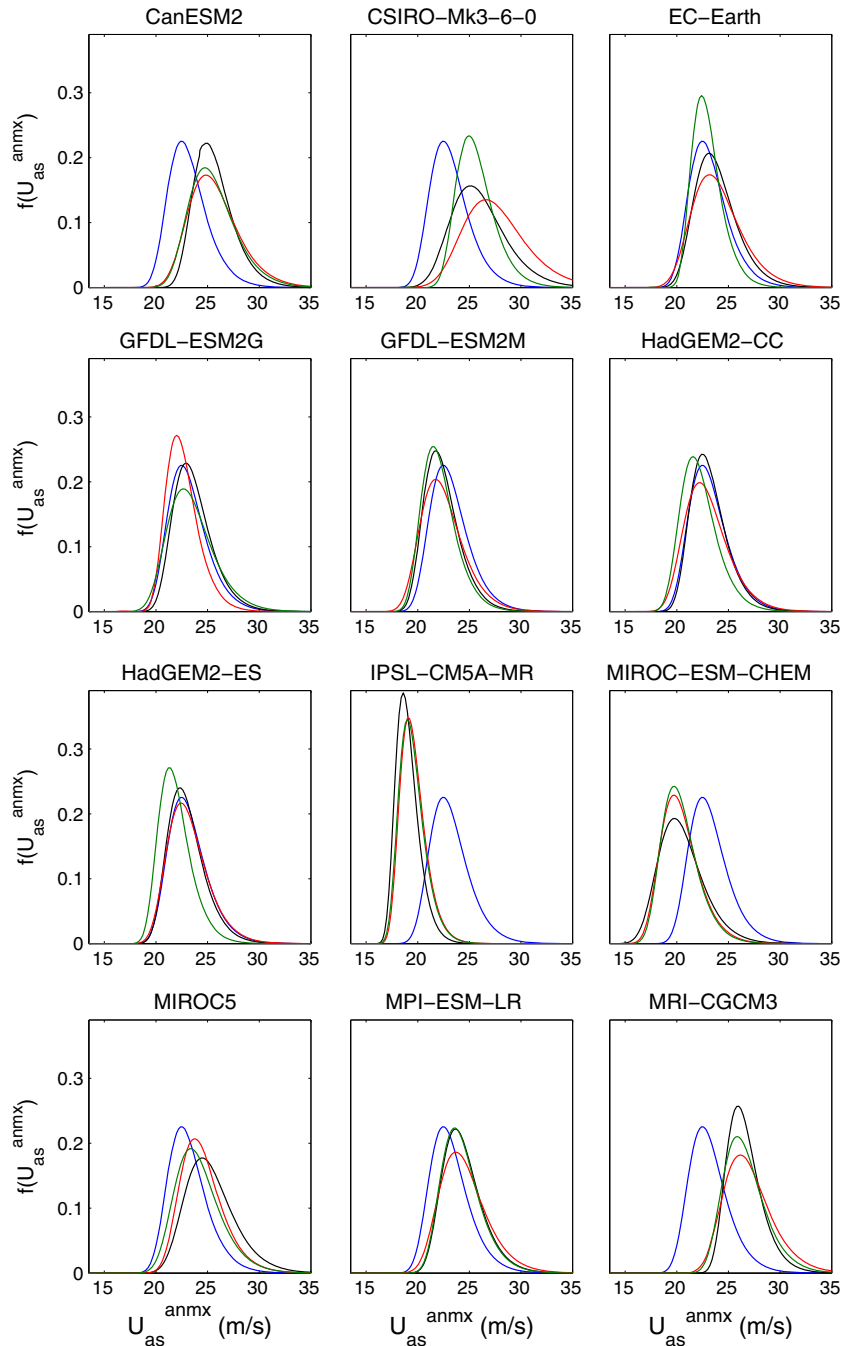
Figure 8. The Gumbel PDFs of U_{as}^{anmx} for ERA-Interim, blue; the historical period, black; and the two scenarios, rcp4.5, red; and rcp8.5, green in the northern box.

where the U_{as}^{anmx} of rcp4.5 is higher than the projections for the historical run. This might be influenced by the number of available members, because, for the historical run, five members were used relative to one member for the two future runs. The confidence interval of the historical run is therefore much smaller than those of the future scenarios.

[24] Except for three models, the return values of U_{as}^{anmx} for a 1:500 year event do not change significantly, as the 95% confidence levels of the future scenarios overlap with those of the historical period (Figures 4 and 5). In the northern box, CanESM2 projects a small (2 m/s), but statistically significant increase in the 1:500 year return wind speed. In contrast, CSIRO-Mk3-6-0 projects the 1:500 year return level for rcp8.5 to decrease in the northern area. This, again, might be the result of the different number of ensemble members in the historical and the future runs. For the southern box, MRI-CGCM3 projects a statistically significant increase of 6 m/s. Although some models project significant changes in the 1:500 year return value of U_{as}^{anmx}, the majority of the 12 GCMs project no significant changes in U_{as}^{anmx} and the corresponding 1:500 year return value.
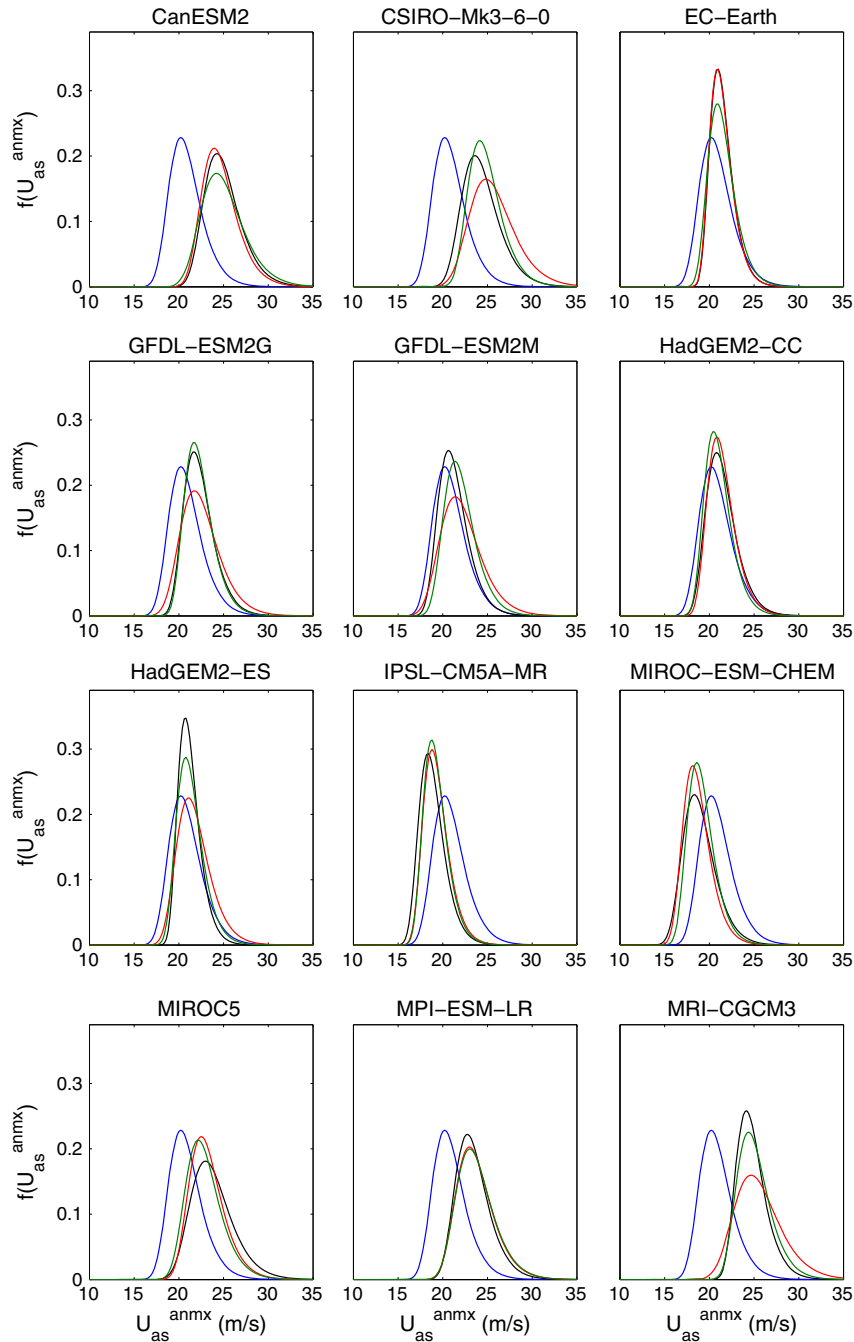
Figure 9. As Figure 8, now for southern box.

3.3. Changes in Wind Direction

[25] The difference in $\%_{wind}$ per direction between the historical run and the two future runs are given in Figures 10 and 11 for the northern and southern location, respectively. The colors represent the different models. A measure of the statistical uncertainty is provided by means of the sd of the historical runs (in gray). It is obvious from both figures that the projected changes are small compared to sd of the historical run. Figure 6 depicts the $\%_{wind}$ for the historical run, the changes shown in Figures 10 and 11 are substantial relative to these historical $\%_{wind}$. The change in wind direction at both locations shows

a tendency towards less U_{as}^{anmx} from south-eastern directions and more U_{as}^{anmx} from south-western and western directions. The $\%_{wind}$ are based on 50 to 250 values per model–scenario combination; we estimated sd of these $\%_{wind}$ with bootstrapping. The limited amount of years makes it hard to statistically establish changes in the U_{as}^{anmx} direction. The change from southeasterly to more south-western and western winds may point to a poleward shift in storm tracks, because for a given location in the North Sea, a storm that passes to the north causes predominantly westerly winds, while a storm that passes to the south produces mainly southeastern winds. The suggested shift
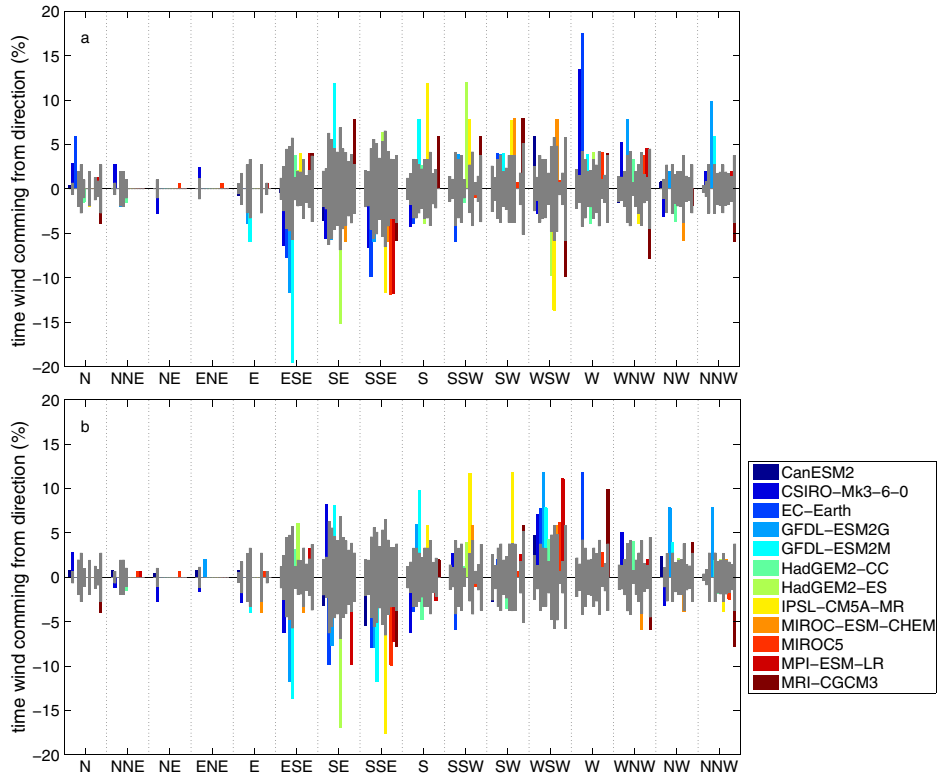
Figure 10. Changes in %$_{wind}$ that U_{as}^{anmx} is projected to come from a certain direction. (a) %$_{wind}$ rcp4.5 - %$_{wind}$ historical, (b) %$_{wind}$ rcp8.5 - %$_{wind}$ historical. In gray, the *sd* of the historical run is depicted as indication of the statistical uncertainty.
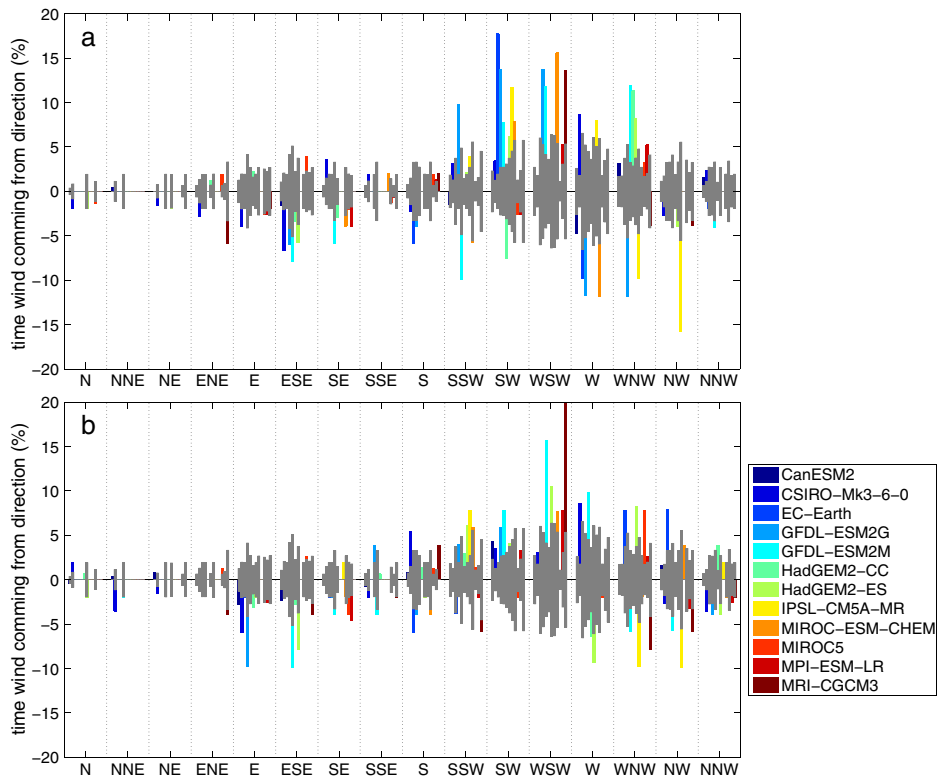

Figure 11. As Figure 10, now for southern box.

in storm tracks is consisted with *Bengtsson et al.* [2006] for CMIP3 GCMs and for CMIP5 GCMs by *Harvey et al.* [2012] and *Chang et al.* [2012].

4. Discussion

[26] As mentioned in section 1, there are three types of uncertainty when analyzing changes in a changing climate [*Hawkins and Sutton*, 2009]. Uncertainty exists in the emission scenarios and the corresponding rcps, in the GCMs and because of the natural variability within the climate system. We were able to address the first two uncertainties by analyzing two climate scenarios for 12 CMIP5 GCMs. We analyzed changes in U_{as}^{anmx} and the corresponding wind direction. U_{as}^{anmx} has large natural variability; this was not reduced for GCMs where multiple ensembles were available, as indicated by the 95% confidence levels in Figures 4 and 5. The 95% confidence levels for models with multiple members are relatively small, although this is also the case for some models with one member. For the CMIP5 models we used, we do not find changes in U_{as}^{anmx} and in the return values of U_{as}^{anmx}, as the models do not produce consistent changes. Furthermore, we see an indication that U_{as}^{anmx} is coming more often from western directions, in line with the studies based on CMIP3 models (section 1).

[27] From a coastal safety perspective, the shift toward more westerly directions for U_{as}^{anmx} is particularly relevant for the German Bight, as such a shift creates larger extreme waves and surge levels [*Woth et al.*, 2006; *Weisse and Günther*, 2007; *Grabemann and Weisse*, 2008]. For the Dutch coast, however, such a directional change in wind direction barely affects surge levels [*Sterl et al.*, 2009] and the annual maximum wave period and height [*De Winter et al.*, 2012].

[28] It should be noted that the models available in CMIP5 have a relatively coarse resolution, roughly between 1° and 3° (Table 1), and are therefore not able to resolve tropical cyclones [*Solomon et al.*, 2007]. A high-resolution run of EC-Earth, Haarsma (personal communication) shows that tropical cyclones might affect the North Sea basin, with U_{as} exceeding 12 Bf (>32.6 m/s); how these extreme wind and the possible shift in U_{as}^{anmx} wind directions, in combination with accelerated sea level rise, will affect coastal safety, is a topic for future study.

5. Conclusions

[29] We examined the changes in U_{as}^{anmx} and corresponding wind directions as a result of climate change for the North Sea basin, using 12 GCMs from the CMIP5 ensemble. To this end, we compared historical runs, running from 1950 to 2000, with two future climate scenarios, rcp4.5 and rcp8.5, running from 2050 to 2100. Consistent with ERA-Interim results, U_{as}^{anmx} in the historical run demonstrates large interannual variability. For the two regions in the North Sea we studied, U_{as}^{anmx} is not projected to change in either rcp4.5 or rcp8.5. In fact, the differences between the 12 GCMs are larger than the difference between the historical and two future runs. Furthermore, the majority of the 12 GCMs shows no statistically significant change in the magnitude of wind extremes up to 1:500 years, for both scenarios.

[30] The variation in direction of U_{as}^{anmx} is large, and this precludes a firm statement on climate-change-induced changes in these directions. Nonetheless, most models

indicate a decrease in U_{as}^{anmx} from south-eastern directions and an increase from south-western and western directions, compatible with a poleward shift of the storm track. The amount of wind from north-west and north-north-west, wind directions that are responsible for the development of extreme storm surges in the southern part of the North Sea, are not projected to change. The results of the CMIP5 models we diagnosed reaffirm results of the CMIP3 models.

References

Alexandersson, H., T. Schmith, K. Iden, and H. Tuomenvirta (1998), Long-term variations of the storm climate over NW Europe, *Global Atmos. Ocean Syst.*, *6*(2), 97–120.

Alexandersson, H., H. Tuomenvirta, T. Schmith, and K. Iden (2000), Trends of storms in NW Europe derived from an updated pressure data set, *Climate Res.*, *14*(1), 71–73.

Bengtsson, L., K. I. Hodges, and E. Roeckner (2006), Storm tracks and climate change, *J. Climate*, *19*(15), 3518–3543, doi:10.1175/JCLI3815.1.

Chang, E. K. M., Y. Guo, and X. Xia (2012), CMIP5 multimodel ensemble projection of storm track change under global warming, *J. Geophys. Res.*, *117*(D23), 118, doi:10.1029/2012JD018578.

Coles, S. (2001), An Introduction to Statistical Modeling of Extreme Values, pp. 45–73, Springer-Verlag, London, Berlin, Heidelberg.

Compo, G. P., et al. (2011), The twentieth century reanalysis project, *Q. J. Roy. Meteor. Soc.*, *137*(654), 1–28, doi:10.1002/qj.776.

De Winter, R. C., A. Sterl, J. W. de Vries, S. L. Weber, and B. G. Ruessink (2012), The effect of climate change on extreme waves in front of the Dutch coast, *Ocean Dynam.*, 1139–1152, doi:10.1007/s10236-012-0551-7.

Dee, D. P., et al. (2011), The ERA-Interim reanalysis: Configuration and performance of the data assimilation system, *Q. J. Roy. Meteor. Soc.*, *137*(656), 553–597, doi:10.1002/qj.828.

Donat, M. G., D. Renggli, S. Wild, L. V. Alexander, G. C. Leckebusch, and U. Ulbrich (2011), Reanalysis suggests long-term upward trends in European storminess since 1871, *Geophys. Res. Lett.*, *38*(14), doi:10.1029/2011GL047995.

Grabemann, I., and R. Weisse (2008), Climate change impact on extreme wave conditions in the North Sea: An ensemble study, *Ocean Dynam.*, *58*, 199–212, doi:10.1007/s10236-008-0141-x.

Harvey, B. J., L. C. Shaffrey, T. J. Woollings, G. Zappa, and K. I. Hodges (2012), How large are projected 21st century storm track changes, *Geophys. Res. Lett.*, *39*(17), L18,707, doi:10.1029/2012GL052873.

Hawkins, E., and R. Sutton (2009), The potential to narrow uncertainty in regional climate predictions, *Bull. Amer. Meteor. Soc.*, *90*(8), 1095–1107, doi:10.1175/2009BAMS2607.1.

Meinshausen, M., et al. (2011), The RCP greenhouse gas concentrations and their extensions from 1765 to 2300, *Clim. Chang.*, *109*(1), 213–241, doi:10.1007/s10584-011-0156-z.

Nikulin, G., E. Kjellström, U. Hansson, G. Strandberg, and A. Ullerstig (2011), Evaluation and future projections of temperature, precipitation and wind extremes over Europe in an ensemble of regional climate simulations, *Tellus A*, *63*(1), 41–55, doi:10.1111/j.1600-0870.2010.00466.x.

Parry, M. L., O. F. Canziani, J. P. Palutikof, P. J. van der Linden, and C. E. Hanson (2007), Contribution of Working Group II to the Fourth Assessment Report of the Intergovernmental Panel on Climate Change, Cambridge University Press, Cambridge, United Kingdom and New York, NY, USA, 976 pp.

Pryor, S. C., R. J. Barthelmie, N. E. Clausen, M. Drews, N. MacKellar, and E. Kjellström (2012), Analyses of possible changes in intense and extreme wind speeds over northern Europe under climate change scenarios, *Clim. Dynam.*, *38*(1-2), 189–208, doi:10.1007/s00382-010-0955-3.

Solomon, S., D. Qin, M. Manning, Z. Chen, M. Marquis, K. Averyt, M. Tignor, and H. Miller (2007), Contribution of Working Group I to

the Fourth Assessment Report of the Intergovernmental Panel on Climate Change, 996 pp., Cambridge University Press, Cambridge, United Kingdom and New York, NY, USA.

Sterl, A., H. Van den Brink, H. De Vries, R. Haarsma, and R. van Meijgaard (2009), An ensemble study of extreme storm surge related water levels in the North Sea in a changing climate, *Ocean Sci.*, *5*, 369.

The WASA-Group (1998), Changing waves and storms in the northeast Atlantic?, *Bull. Amer. Meteor. Soc.*, *79*, 741–760.

Van den Brink, H. W., and G. P. Können (2008), The statistical distribution of meteorological outliers, *Geophys. Res. Lett.*, *35*(23), doi:10.1029/2008GL035967.

Van den Hurk, B., et al. (2007), New climate change scenarios for the Netherlands, *Water Sci. Technol.*, *56*(4), 27–33, doi:10.2166/wst.2007.533.

Von Storch, H., and F. W. Zwiers (2001), Statistical Analysis in Climate Research, 117–118 pp., Cambridge University Press, Cambridge, UK.

Wang, X. L., H. Wan, F. W. Zwiers, V. R. Swail, G. P. Compo, R. J. Allan, R. S. Vose, S. Jourdain, and X. Yin (2011), Trends and low-frequency variability of storminess over western Europe, 1878-2007, *Clim. Dynam.*, *37*(11-12), 2355–2371, doi:10.1007/s00382-011-1107-0.

Weisse, R., and H. Günther (2007), Wave climate and long-term changes for the Southern North Sea obtained from a high-resolution hindcast 1958-2002, *Ocean Dynam.*, *57*(3), 161–172, doi:10.1007/s10236-006-0094-x.

Woth, K., R. Weisse, and H. Von Storch (2006), Climate change and north sea storm surge extremes: An ensemble study of storm surge extremes expected in a changed climate projected by four different regional climate models, *Ocean Dynam.*, *56*(1), 3–15, doi:10.1007/s10236-005-0024-3.